Electronic Supplementary Material (ESI) for Journal of Materials Chemistry A.
This journal is © The Royal Society of Chemistry 2023

Supporting Information

Synchronous stabilization of Li-S electrodes by 1T MoS_2@AAO functional interlayer

Binchao Shi, Yue Wang, Ertai Liu, Shilin Mei,* and Chang-Jiang Yao*

State Key Laboratory of Explosion Science and Technology, Beijing Institute of Technology, Beijing 100081 P. R. China.

* E-mail: shilin.mei@bit.edu.cn; cjyao@bit.edu.cn

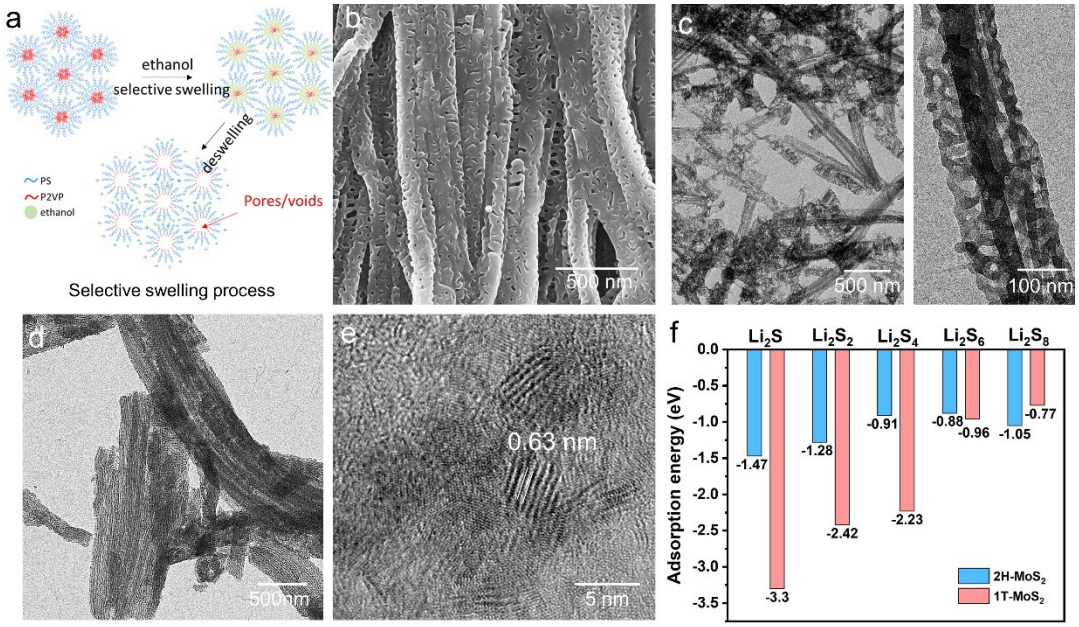

Figure S1. (a) The schematic picture of selective swelling process. (b) SEM images of PS-*b*-P2VP nanotubes. (c) TEM images of the PS-P2VP porous structures. (d) Low resolution TEM images of the MoS_2 nanotubes after dissolving AAO. (e) High resolution TEM images of the MoS_2 tubes after dissolving AAO. (f) Calculated adsorption energy of 1T and 2H phase MoS_2 to lithium polysulfides in previous research.

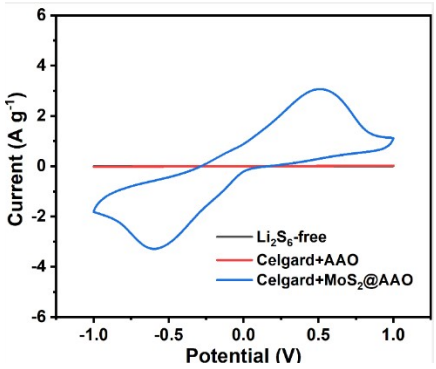

Figure S2. CV curves at a scan rate of 10 mV s^{-1} from -1.0 to 1.0 V of the symmetric batteries with different electrodes with and without the presence of Li_2S_6.

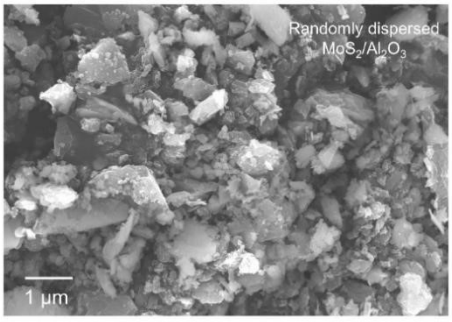

Figure S3. SEM images of randomly mixed MoS_2/Al_2O_3 without the vertical channels.

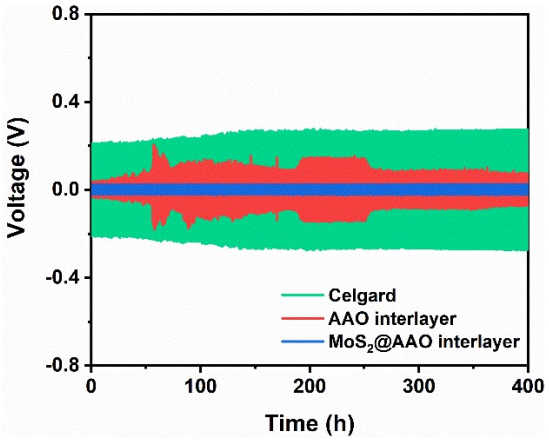

Figure S4. Voltage profile of the three symmetric cells at 5 mAh cm^{-2}.

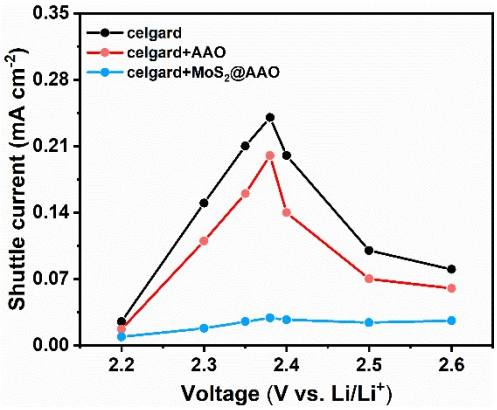

Figure S5. The shuttle currents of Li–S cells with Celgard, Celgard+AAO, and Celgard +MoS_2@AAO.

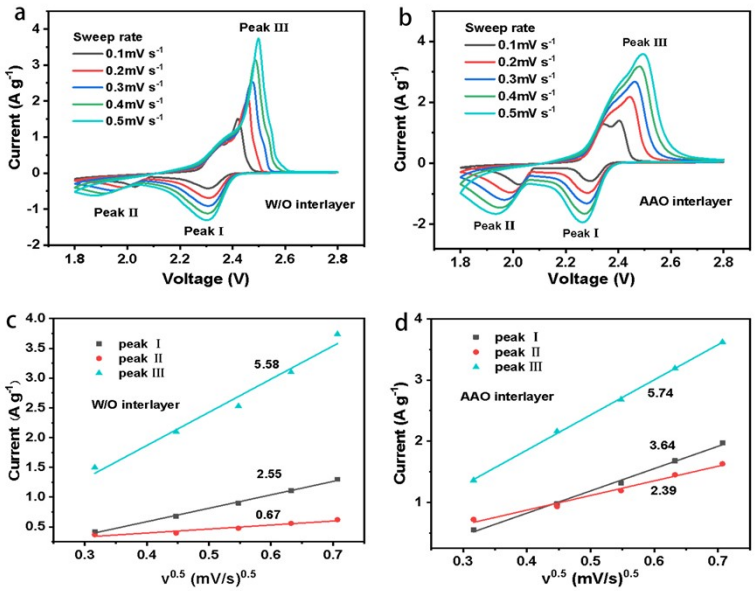

Figure S6. CV curves (a, b) and redox peak current dependence on the square root of the scan rate (c, d) of batteries based on Celgard, Celgard with AAO at different scan rate from 0.1 mV s^{-1} to 0.5 mV s^{-1}.

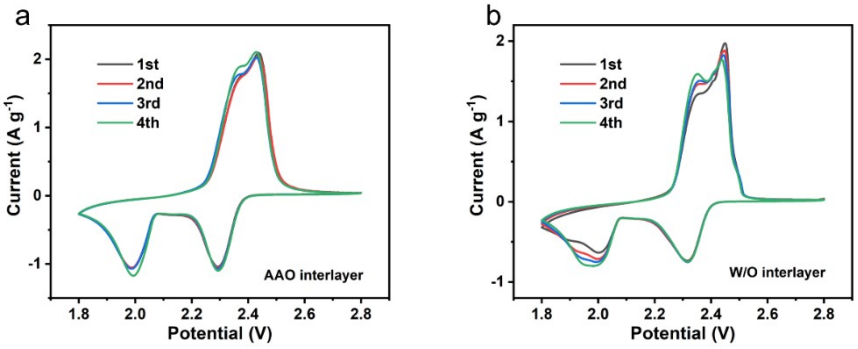

Figure S7. CV curves of different Li-S battery. Celgard with AAO (a) and Celgard (b) at 0.2 mV s^{-1}.

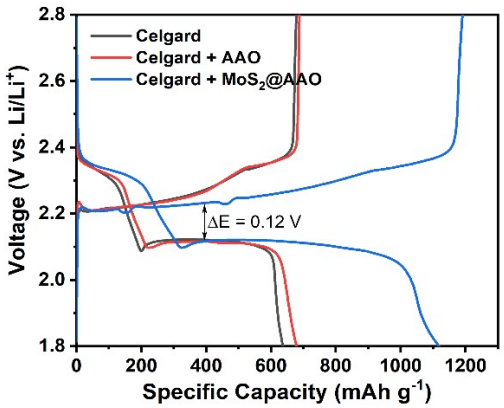

Figure S8. Charge/discharge profiles of Li-S battery with MoS_2@AAO interlayer (a), Celgard with AAO (b), and Celgard (c) at 0.1 C.

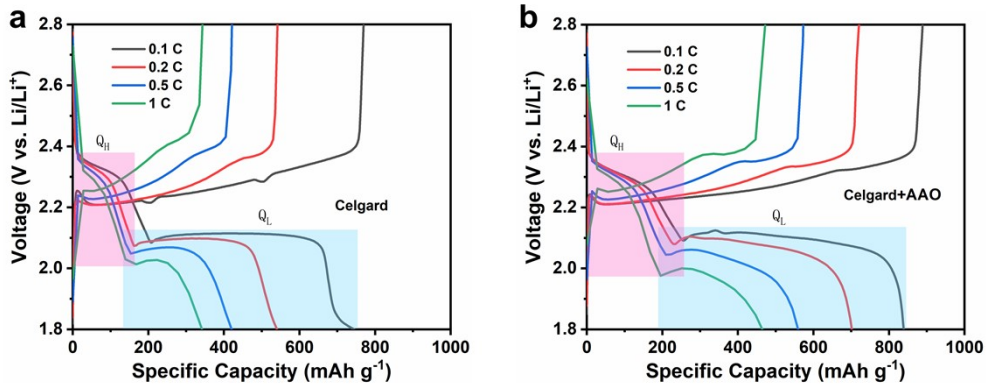

Figure S9. Charge/discharge profiles of Celgard (a) and Celgard with AAO (b) from 0.1 to 1 C.

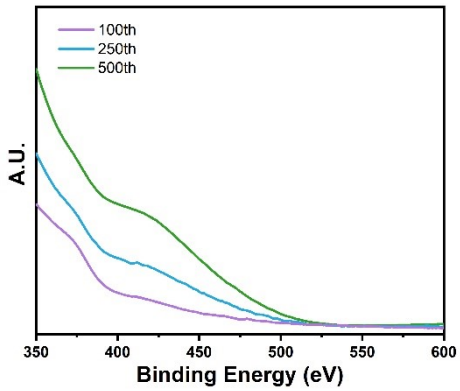

Figure S10. UV-vis spectra of the polysulfides released from the cycled MoS2@AAO membranes.

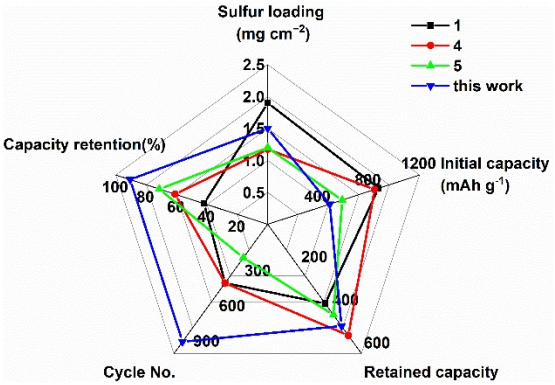

Figure S11. Comparison of the electrochemical performance of recently reported work in Li−S batteries.

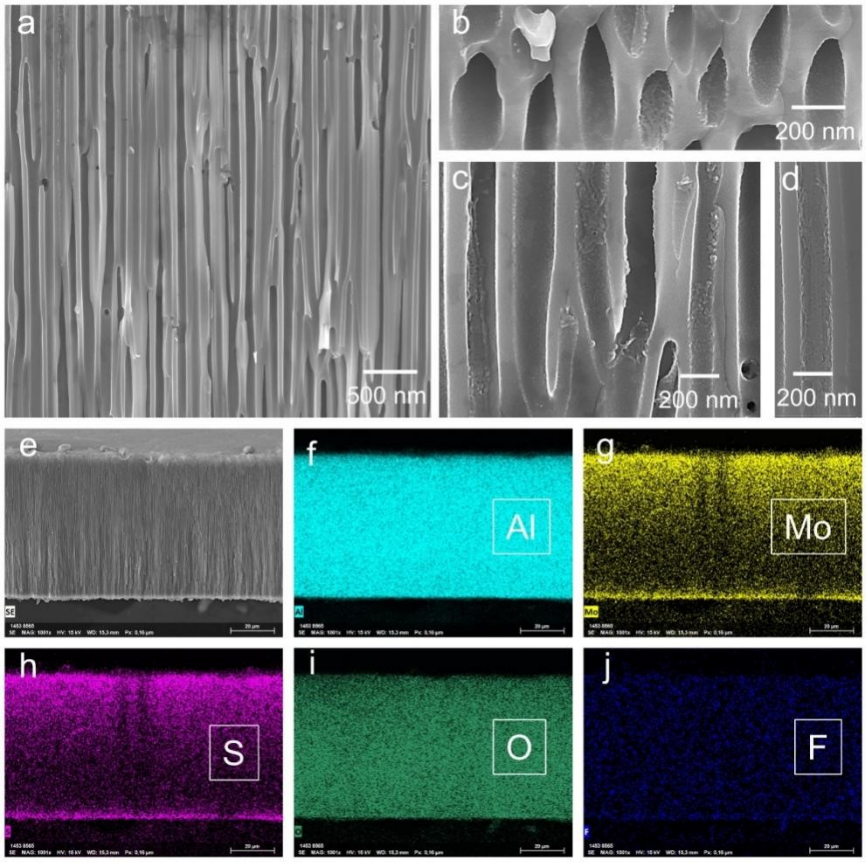

Figure S12. The SEM and the corresponding EDS mapping images of MoS_2@AAO after cycling.

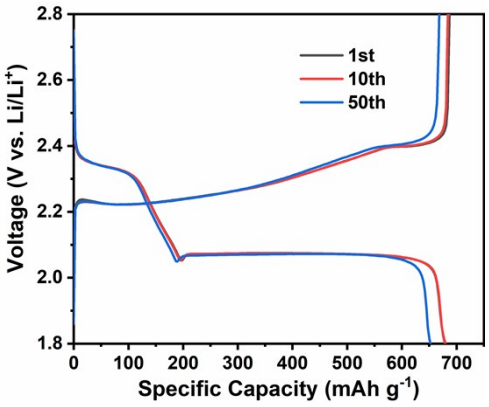

Figure S13. Charge/discharge profiles of Celgard with MoS_2@AAO cells at 0.1 C with a high sulfur loading of =5.0 mg cm^{-2} and E/S=7 μL mg^{-2}.

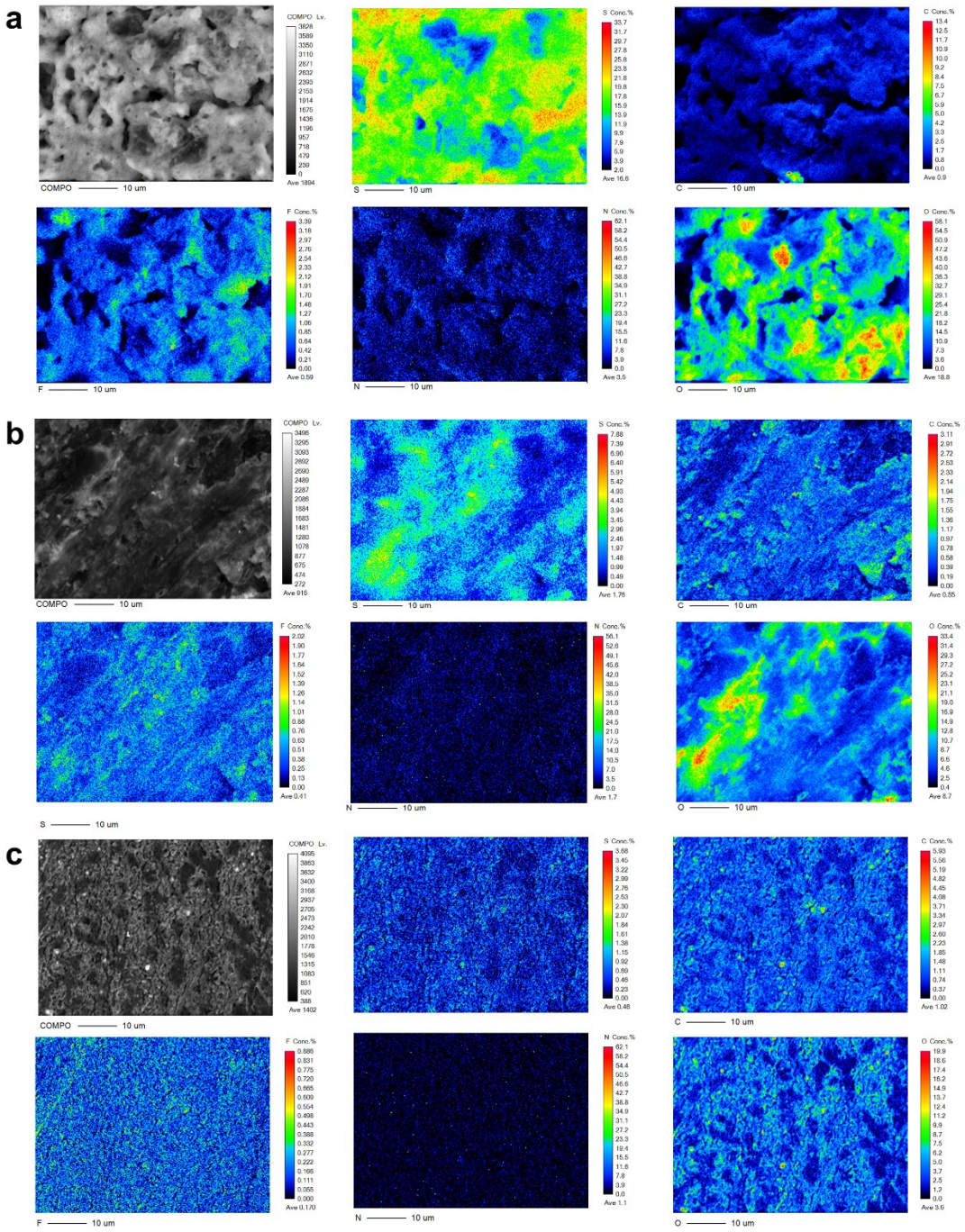

Figure S14. EPMA mapping of the Li anode of (a) Celgard, (b) Celgard with AAO, and (c) Celgard with MoS_2@AAO cells after 50 cycles.

Table S1. A summary of the electrochemical performances of representative works

Interlayer materials	Sulfur loading (mg cm^{-2})	Initial/highest capacity (mAh g^{-1})	Retained capacity (mAh g^{-1})	Cycle number	Capacity retention (%)	C rate	Ref.
rGO@MoS_2	1.8-2.0	1121	671	200	59.8	0.2 C	1
		877	368	500	42.0	1 C	
MoS_2/CNT	1.4	1250	770	200	61.6	0.2 C	2
		1237	648	500	52.4	0.5 C	
MoS_2@CMT	1.0	1133	765	500	67.5	0.5 C	3
CNNFs-MoS_2/PP	1.1-1.25	845.4	515.7	500	61.0	1 C	4
AAO	1.2	1334.7	958.4	100	71.8	0.2 C	5
		589.6	421.2	285	71.4	1 C	
MoS_2@AAO	**1.5**	**901**	**897**	**500**	**99.6**	**0.2 C**	**This work**
		491	**472**	**1000**	**90.6**	**1 C**	

References:

[1] L. Tan, X. Li, Z. Wang, H. Guo, J. Wang, *ACS Appl. Mater. Interfaces* **2018**, *10*, 3707.

[2] L. Yan, N. Luo, W. Kong, S. Luo, H. Wu, K. Jiang, Q. Li, S. Fan, W. Duan, J. Wang, *J. Power Sources* **2018**, *389*, 169.

[3] J. Yang, L. Yu, B. Zheng, N. Li, J. Xi, X. Qiu, *Advanced Science* **2020**, *7*, 1903260.

[4] K. Gao, D. Xia, H. Ji, Y. Chen, L. Zhang, Y. Wang, S. Yi, Y. Zhou, Z. Zhang, D. Chen, Y. Gao, *Energy Fuels* **2021**, *35*, 10303.

[5] B. Wang, W. Guo, Y. Fu, *ACS Appl. Mater. Interfaces* **2020**, *12*, 5831.